Journal of Visualized Experiments

Preparation of Tunable Extracellular Matrix Microenvironments to Evaluate Schwann Cell Phenotype Specification

--Manuscript Draft--

Article Type:	Invited Methods Article - JoVE Produced Video
Manuscript Number:	JoVE61496R1
Full Title:	Preparation of Tunable Extracellular Matrix Microenvironments to Evaluate Schwann Cell Phenotype Specification
Section/Category:	JoVE Bioengineering
Keywords:	Schwann cells; peripheral nerve; matrix stiffness; extracellular matrix; micropatterning; cell phenotype; plasticity; cell shape
Corresponding Author:	Greg Harris, Ph.D. UNITED STATES
Corresponding Author's Institution:	
Corresponding Author E-Mail:	harrigy@ucmail.uc.edu
Order of Authors:	Zhenyuan Xu
	Jacob A. Orkwis
	Greg M. Harris, Ph.D.
Additional Information:	
Question	**Response**
Please indicate whether this article will be Standard Access or Open Access.	Standard Access (US$2,400)
Please indicate the **city, state/province, and country** where this article will be **filmed**. Please do not use abbreviations.	Cincinnati, Ohio, United States

University of CINCINNATI

Greg M. Harris, Ph.D.
Assistant Professor
Department of Chemical Engineering
University of Cincinnati
Phone: 513-556-4167
Email: gregory.harris@uc.edu

May 5, 2020

Kyle Jewhurst, Ph.D.
Science Editor, Journal of Visual Experiments

Dear Dr. Jewhurst,

We are submitting a revised version of our manuscript entitled "Deciphering the Impact of the ECM in Schwann Cell Phenotype Specification" for considered publication in *Journal of Visual Experiments (JoVE)*.

We have performed the experiments and suggestions of the reviewers in the decision letter. Our complete revisions are detailed in the Responses to Reviewers file.

We agree that inclusion of these new additions strengthen our manuscript and hope that our work is now acceptable for publication.

Thank you for considering this manuscript. We look forward to your decision.

Sincerely,

Greg Harris

Greg M. Harris, Ph.D.

TITLE:

Preparation of Tunable Extracellular Matrix Microenvironments to Evaluate Schwann Cell Phenotype Specification

AUTHORS AND AFFILIATIONS:

Zhenyuan Xu[1], Jacob A. Orkwis[1], Greg M. Harris[1,2,3]

[1]Department of Chemical and Environmental Engineering, University of Cincinnati, Cincinnati, OH
[2]Department of Biomedical Engineering, University of Cincinnati, Cincinnati, OH
[3]Neuroscience Graduate Program, University of Cincinnati College of Medicine, Cincinnati, OH

Corresponding author:

Greg M. Harris (gregory.harris@uc.edu)

Co-Authors:

Zhenyuan Xu (xuzy@mail.uc.edu)
Jacob A. Orkwis (orkwisja@mail.uc.edu)

KEYWORDS:

Schwann cells, peripheral nerve, matrix stiffness, extracellular matrix, micropatterning, cell phenotype, plasticity, cell shape

SUMMARY:

This methodology aims to illustrate the mechanisms by which extracellular matrix cues such as substrate stiffness, protein composition and cell morphology regulate Schwann cell (SC) phenotype.

ABSTRACT:

Traumatic peripheral nervous system (PNS) injuries currently lack suitable treatments to regain full functional recovery. Schwann cells (SCs), as the major glial cells of the PNS, play a vital role in promoting PNS regeneration by dedifferentiating into a regenerative cell phenotype following injury. However, the dedifferentiated state of SCs is challenging to maintain through the time-period needed for regeneration and is impacted by changes in the surrounding extracellular matrix (ECM). Therefore, determining the complex interplay between SCs and differing ECM to provide cues of regenerative potential of SCs is essential. To address this, a strategy was created where different ECM proteins were adsorbed onto a tunable polydimethylsiloxane (PDMS) substrate which provided a platform where stiffness and protein composition can be modulated. SCs were seeded onto the tunable substrates and critical cellular functions representing the dynamics of SC phenotype were measured. To illustrate the interplay between SC protein expression and cellular morphology, differing seeding densities of SCs in addition to individual microcontact printed cellular patterns were utilized and characterized by immunofluorescence staining and western blot. Results showed that cells with a smaller spreading area and higher extent of cellular elongation promoted higher levels of SC regenerative phenotypic markers. This methodology not only begins to unravel the significant relationship between the ECM and cellular

function of SCs, but also provides guidelines for the future optimization of biomaterials in peripheral nerve repair.

INTRODUCTION:

Peripheral nervous system (PNS) injuries remain a major clinical challenge in healthcare by compromising the quality of life for patients and creating a significant impact through a multitude of socioeconomic factors[1,2]. Schwann cells (SC), as the major glial cells in the PNS, provide necessary molecular and physical cues to induce PNS regeneration and aid in functional recoveries in short gap injuries. This is due to the remarkable ability of SCs to dedifferentiate into a "repair" cell phenotype from a myelinating or Remak phenotype[3]. The repair SC is a distinctive cell phenotype in several ways. Following injury, SCs increase their proliferation rate by re-entering the cell cycle and begin expression of several transcriptional factors to facilitate reinnervation. These factors, such as c-Jun and p75 NTR, are upregulated while myelinating SC markers, such as myelin basic protein (MBP), are downregulated[4,5]. In addition, SCs change morphology to become elongated and aligned with each other to form Büngner bands across the injury site[6]. This provides a physical guidance mechanism for the axons to extend to the correct distal target[7]. However, despite the ability that SCs possess to promote nerve regeneration in short gap injuries, the outcome of functional recovery remains poor in severe injuries. This is due in part to a loss of extracellular matrix (ECM) guidance cues, as well as the inability of SCs to maintain the regenerative phenotype over long periods of time[8].

The nerve regeneration and recovery process are intimately tied to the state of the basal lamina following injury. The basal lamina is a layer of ECM around the nerve that facilitates guidance and provides ECM-bound cues for axons and SCs in cases where it remains intact following injury[9]. The state of the ECM and its ability to deliver matrix bound cues to cells is vitally important and has been previously explored in a variety of different contexts[10-14]. For example, it has been shown that the stiffness of the ECM can guide cell functions such as proliferation and differentiation[11,15,16]. Composition of the ECM can also lead to a distinct cellular response and regulate cell behaviors such as migration and differentiation through intracellular signaling pathways[17,18]. Furthermore, cell morphology, including spreading area and cellular elongation, play a major role in regulating the function and can be governed by ECM-bound cues[19,20]. Many previous studies have focused on stem cells differentiating into defined lineages, yet SCs possess a similar ability to alter phenotype from a homeostatic, adult SC within a healthy nerve, to a repair SC capable of secreting proteins and growth factors while remodeling the ECM following nerve injury[5,21]. Therefore, it is especially crucial to identify mechanisms underlying the relationship between the innate SC regenerative capacity and ECM bound cues for the insight to ultimately harness this capacity for nerve regeneration.

To address this, we have developed a detailed methodology to produce a cell culture substrate where mechanical stiffness and ligand type can be easily tuned in physiologically relevant ranges. Polydimethyl siloxane (PDMS) was chosen as a substrate due to its highly tunable mechanics as compared to polyacrylamide gel, where the maximum Young's modulus is around 12 kPa contrasted to PDMS at around 1000 kPa[22-24]. This is beneficial to the work at hand, as recent studies have shown the Young's modulus of a rabbit sciatic nerve can exceed 50 kPa during

development, thereby suggesting that the range of stiffness of nerves within the PNS is wider than previously examined. Different proteins are capable of adsorption onto PDMS substrates to analyze the combinatorial regulation of mechanics and ligands on SC behavior. This allows for the investigation of multiple microenvironmental cues present in the PNS regeneration process and comparison of a high degree of tunability to the work focusing solely on stiffness of the substrate[25]. Further, these engineered cell culture substrates are compatible with a multitude of quantitative analysis methods such as immunohistochemistry, western blot, and quantitative polymerase chain reaction (q-PCR).

This engineered cell culture platform is highly suitable for analyzing mechanistic pathways due to the high level of individual tunability of each ECM-bound signal. In addition, popular methods for cell micropatterning, including microcontact printing, can be achieved on the substrates to allow for controlled cellular adhesion to analyze cell shape in relation to other ECM bound cues[24]. This is critical because line patterned substrates, which promote elongation in cell populations, provide a tool to mimic and study elongated and regenerative SCs within Büngner bands during nerve regeneration. Further, cellular morphology is a potent regulator of multiple cell functions and can potentially introduce confounding experimental results if not controlled[26,27]. Significant attention is now being provided to the mechanisms governing the SC regenerative phenotype as regulated by ECM cues[28-30]. This is essential to provide insight into the design of biomaterials that can be applied as nerve guidance conduits for aid in PNS nerve regeneration. These detailed protocols can ultimately be applied as a potential tool to decipher the mechanisms of SC and other cell type function as regulated by ECM bound cues.

PROTOCOL:

1. Tunable cell culture substrate preparation and characterization

1.1. Substrate preparation

1.1.1. Mix the PDMS base elastomer and curing agents using a pipette tip vigorously at a ratio between 10:1 and 60:1 until bubbles are homogeneously dispersed within the mixture. Remove bubbles using vacuum desiccation until bubbles are dissipated.

NOTE: During PDMS polymerization, curing agent crosslinks with the base elastomer to provide final polymer desired mechanical properties. Crosslink ratios can be adjusted to alter PDMS stiffness.

1.1.2. Place a drop (~0.2 mL) of desiccated PDMS mixture on a square or circular coverslip (e.g., 22 mm x 22 mm) and rotate the coverslip on a spin coater at 2500 rpm for 30 s.

1.1.3. Incubate the coverslip in either an oven at 60 °C for 1-2 h or room temperature overnight for PDMS to solidify.

1.1.4. Treat the coverslip using UV-Ozone cleaner for 7 min (UV wavelength: 185 nm and 254 nm)

to increase the surface hydrophilicity. Place it into a sterilized 6-well plate.

1.1.5. Before using for cell culture, incubate substrates in 70% ethanol for at least 30 min.

CAUTION: UV-Ozone cleaner can generate Ozone that is harmful to humans. Work in a chemical fume hood or with some form of ventilation.

1.1.6. Immerse coverslips in the protein solution (10 µg/mL collagen I, fibronectin, or laminin) for 60 min in a sterile incubator at 37 °C.

NOTE: Following UV-Ozone treatment, the PDMS surface may still be hydrophobic. Rotate the well plate to ensure each coverslip is covered with the protein solution.

1.1.7. Aspirate the protein solution and wash the coverslip with phosphate buffered saline (PBS) 3x.

1.1.8. Re-suspend RT4-D6P2T Schwann cell line (SCs) from passaging dish using commercially available EDTA solution (1x) with 2.5% trypsin and count cells with hemocytometer. Seed SCs on the tunable PDMS surface at the desired cell density. SC seeding densities may vary for each different application.

1.1.9. Maintain cells in the desired cell culture parameters (90% humidity, 5% CO_2, 37 °C, etc.) for the length of experiment. Use Dulbecco's Modified Eagle Medium (DMEM) supplemented with 10% fetal bovine serum (FBS) and 1% penicillin-streptomycin as the cell culture medium.

1.2. Micropatterned substrate preparation

1.2.1. Draw the desired geometry and cell adhesive areas (900 μm^2, 1,600 μm^2 and 2,500 μm^2) using computer-aided design (CAD) software. Create a chrome photomask based on those patterns from a commercial supplier.

1.2.2. In a clean room or dust free environment, use standard photolithography techniques to fabricate silicon wafers (protocols are detailed elsewhere[31]). Critical parameters for this particular application are as follows: Photoresist: SU-8 2010; Spin profile to disperse the photoresist: 500 rpm for 10 s with an acceleration of 100 rpm/s, then 3500 rpm for 30 s with an acceleration of 300 rpm/s; Exposure energy of UV light: 130 mJ/cm^2.

NOTE: The height of patterns on the silicon wafers is approximately 10 µm following these parameters. Potential cracks around the edge outside of the rectangular or triangular patterns can be seen using a light microscope after step 1.2.2. Baking the silicon wafer at 190 °C for 30 min helps to eliminate the cracks.

1.2.3. Place the patterned silicon wafer inside a circular 150 mm diameter x 15 mm height Petri dish and pour de-gassed PDMS (mixing ratio 10:1) as prepared in step 1.1.1 onto the silicon wafer.

NOTE: Ensure the thickness of PDMS is at least 5 mm for ease of handling during microcontact printing steps.

1.2.4. Solidify PDMS on silicon wafer in an oven at 60 °C overnight. Allow PDMS to cool to room temperature. Precisely cut stamps of 30 mm x 30 mm squares containing the correct patterns from the silicon wafer using a surgical scalpel. Do not damage the silicon wafer.

NOTE: Silicon wafers can be reused many times at this point to produce more stamps following cleaning with isopropanol.

1.2.5. Sterilize PDMS stamps and the tunable coverslips (prepared in step 1.1.1 to 1.1.3) by immersing them into 70% ethanol for 30 min.

1.2.6. To confirm the efficacy of micropattern by PDMS stamps after microcontact printing, dry the surface of PDMS stamps using a filtered air stream and pipette 50 µg/mL BSA (Texas Red conjugated) solution to cover the entire patterned side of the PDMS stamp.

1.2.7. Incubate PDMS stamps with BSA solution for 1 h at room temperature to allow for protein adsorption.

1.2.8. Dry the surface of tunable coverslips using a filtered air stream, increase surface hydrophilicity as described in step 1.1.5.

1.2.9. Air dry the PDMS stamps to remove the remaining BSA solution.

NOTE: Take care that BSA solution is completely removed from the stamp because any remaining solution will cause stamps to slide on the coverslip during microcontact printing.

1.2.10. Bring the patterned side of the stamp into conformal contact with the tunable coverslip for BSA adsorption on the coverslip surface. Gently press the stamp against the coverslip for 5 min.

NOTE: Do not apply excessive force on the stamp since it will bend and cause non-specific contact between stamp and coverslip. The appropriate amount of force applied on the stamp is essential for successful microcontact printing.

1.2.11. Examine the micropattern using fluorescence microscope with a FITC (Fluorescein isothiocyanate) filter.

1.2.12. To print cell adhesive areas rather than fluorescent patterns, substitute laminin for BSA protein and repeat step 1.2.5 to 1.2.10.

1.2.13. Remove stamps from coverslips, transfer coverslips into a sterilized 6-well plate. Add 2 mL of 0.2% w/v Pluronic F-127 solution into each well to cover the surface of the coverslip and incubate for 1 h at room temperature.

NOTE: Pluronic F-127 can be adsorbed to PDMS surface increasing the hydrophobicity of PDMS surface to block cells from adhesion.

1.2.14. Aspirate Pluronic F-127 solution and wash 5x with PBS and 1x with the cell culture medium before seeding cells. A typical seeding density for SCs is 1,000 cells/cm^2.

1.2.15. 45 min following cell seeding, remove the cell culture medium and wash coverslips with PBS 2x to prevent multiple SCs from adhering to the same pattern. Maintain cells in desired cell culture environment for 48 h before quantification.

1.2.16. To create line-patterned cell culture substrates to examine aligned cells, follow step 1.2.1 to 1.2.4 to create stamps for microcontact printing.

NOTE: The dimensions of the groove/ridge of the lined patterns on stamp is 50 µm x 50 µm for the cells outlined. The total dimensions of the stamp are 10 mm x 10 mm.

1.2.17. Cut stamps into dimensions containing only desired line patterns.

NOTE: When creating stamps in CAD, the unpatterned area of the stamp around the line patterns will correspond to cell adhesive area following microcontact printing. Thus, it is necessary to eliminate unpatterned areas when cutting out the stamp to ensure every SC seeded on the surface follows the patterns.

1.2.18. Follow step 1.1.1 to 1.1.3 to prepare tunable PDMS surface coating two Petri dishes.

NOTE: This will be PDMS covering the Petri dish surface itself and not on a coverslip.

1.2.19. Follow step 1.2.5 to 1.2.10 to perform microcontact printing to print line-patterned cell adhesive areas on one of the PDMS coated Petri dishes.

NOTE: The surface area of a 60 mm x 15 mm Petri dish can contain line-patterned areas from 6 PDMS stamps.

1.2.20. Remove stamps and fill the Petri dish with 4 mL of 0.2% w/v Pluronic F-127 solution and incubate for 1 h.

1.2.21. After microcontact printing, rinse each side of the PDMS stamps with 70% ethanol 3x and dry with air. Rotate PDMS stamps and follow step 1.2.5 to 1.2.10 to print unpatterned cell adhesive area using the unpatterned side of the stamp on the second Petri dish. Repeat step 1.2.13.

1.2.22. Aspirate F-127 solution from dishes, wash 3x with PBS followed with 1x wash using fresh cell culture medium. Seed SCs on dishes.

NOTE: The seeding density for a line-patterned dish is 5,000 cells/cm^2 and for an unpatterned dish is 10,000 cells/cm^2.

1.2.23. Maintain SCs at desired conditions for 48 h and follow protocols to prepare SC lysates[32].

NOTE: The cell seeding density for unpatterned dishes is 2x higher than that for line-patterned dishes, as the line-patterned dish has only half the cell adhesive area of the unpatterned dish.

1.2.23.1. To prepare lysates, transfer adequate radioimmunoprecipitation assay (RIPA) buffer to a 10 mL conical centrifuge tube. Dilute protease and phosphatase inhibitor (100x) at a ratio of 1:100 in RIPA buffer, mix well by pipetting.

1.2.23.2. Wash cells with ice cold PBS (1x) for 2 min, add 80 µL of the solution prepared from step 1.2.23.1 onto each cell adhesive area (the area that contacted with PDMS stamps and adsorbed protein) within petri dishes. Incubate cells with the solution on an ice block for 15 min.

NOTE: The solution will only stay on cell adhesive area due to the hydrophobicity of Pluronic F-127 adsorption elsewhere. This feature enables a successful and sufficient protein extraction for line patterned SCs.

1.2.23.3. Scrape SCs with a cell scraper for 5 min. Collect lysate into a labeled 1.5 mL microcentrifuge tube.

1.2.23.4. Microcentrifuge lysate at 12, 000 *x g* for 15 min at 4°C. Collect supernatant with a 1,000 µL pipette and transfer to a clean microcentrifuge tube. Store cell lysate at -20 °C.

1.3. Substrate characterization

NOTE: To characterize mechanics of the polymer on the coverslip, multiple methods are generally employed including bulk compression testing[11,33] or atomic force microscopy testing[34]. This protocol will outline bulk compression testing.

1.3.1. Pour the PDMS precursor of the desired mixing ratio (step 1.1) into a 30 mm Petri dish, ensure the thickness of the PDMS layer within the Petri dish is at least 20 mm.

1.3.2. Remove the Petri dish with solidified PDMS from 60 °C oven after 1 h and allow to cool at room temperature. Cut polymer into 10 mm x 10 mm squares. Measure the thickness of PDMS using calipers.

1.3.3. Place PDMS on stage of the compression force measuring machine. Plug in compression force sensor (model: 112C) to sensor port and fix the sensor to the axis of the test machine.

1.3.4. Adjust the height of the sensor to approximately 0.5 cm above the PDMS stamp using "jog" control on front panel of instrument.

1.3.5. Open the associated software using "**Test Setup**" window, select "**Servo profile**", and open the "**Segment**" window. In the "**Segment**" window, input desired "**Control Rate**" and "**End Amount**" for the test.

NOTE: Control rate determines the rate at which the sensor travels down towards the PDMS. End amount determines the total distance the sensor travels.

1.3.6. Use the "**Z**" button located on control panel of the software to reset all measurements at this point.

1.3.7. Move the sensor down to lightly contact PDMS until 1-2 newtons (N) are loaded. The loading and the distance that the sensor travels will be displayed in the software.

1.3.8. After utilizing the "**Z**" button, run measurement using "**Play**", and save the file recording force and distance.

1.3.9. Repeat steps 1.3.3 to 1.3.8 for each experimental condition of PDMS.

1.3.10. Open the file and use the following formula to calculate the Young's modulus (E) of PDMS for each ratio. (F = compression force, A = area of PDMS stamp, ΔL = traveling distance of sensor, and L_0 = original thickness of the PDMS stamp).

$$E = \frac{F/A}{\Delta L/L_0}$$

2. Quantification of cellular properties on tunable substrates

2.1. Proliferation assay

2.1.1. Seed SCs on substrates prepared from step 1.1.9 at a density of 5,000 cells/cm^2 in a 6-well plate. Allow SCs to incubate for 48 h in standard cell culture conditions (37 °C and 5% CO_2).

2.1.2. Dilute 12 µL of 10 mM Bromodeoxyuridine (BrdU) stock solution into 12 mL of 37 °C cell culture medium, mix well with pipette to make 10 µM BrdU labeling solution.

2.1.3. Remove the cell culture medium and wash SCs 2x with PBS.

2.1.4. Add 2 mL of BrdU labeling solution into each well and incubate SCs for 2 h.

NOTE: The incubation time of BrdU labeling solution depends on the specific cell proliferation rate. The RT4-D6P2T SC line has a high proliferation rate so 2 h of incubation time was used.

2.1.5. Remove BrdU labeling solution and wash SCs 3x with PBS. Add 1 mL of 3.7% formaldehyde in PBS to each well and incubate at room temperature for 15 min for cell fixation.

CAUTION: Formaldehyde is a human carcinogen; therefore, carry out all work inside a chemical fume hood with appropriate protection.

NOTE: When washing with PBS, there is no cell culture medium in the well, and thus the PDMS surface may be hydrophobic. Take precautions to not completely dry the surface of the substrate to prevent cell damage.

2.1.6. Aspirate formaldehyde solution and wash 3x with PBS (3 min each). Remove PBS and add 1 mL of 0.2% Triton X-100 in PBS to each well to permeabilize cell membrane. Incubate SCs with Triton X-100 solution for 20 min at room temperature.

2.1.7. Remove Triton X-100 solution and wash SCs 3x with PBS (3 min each).

2.1.8. Add 1 mL of 1 N HCl into each well and incubate on ice for 10 min. Remove 1 N HCl and add 1 mL of 2 N HCl into each well and incubate at room temperature for 10 min. HCl treatment is for DNA hydrolysis.

2.1.9. Mix 182 mL of 0.2 mM Na_2HPO_4 and 18 mL of 0.1 mM citric acid to produce a phosphate/citric acid buffer for antigen retrieval. Remove 2 N HCl and add 1 mL phosphate/citric acid buffer into each well and incubate at room temperature for 10 min.

2.1.10. Wash SCs 3x with 0.2% Triton X-100 in PBS. Add 2 mL of 3% bovine serum albumin (BSA) in PBS into each well and incubate for 30 min at room temperature to clock nonspecific binding of the antibody.

2.1.11. Dilute BrdU primary antibody conjugated with Alexa Fluor 488 in 3% BSA solution at a ratio of 1:300 for BrdU staining solution. Incubate SCs with staining solution overnight at room temperature while plate is covered in aluminum foil.

2.1.12. To quantify proliferation, image SCs using the FITC and DAPI channel of a fluorescent microscope to detect BrdU and nuclei, respectively. Save images as “nd.2” files.

2.1.13. Open “nd.2” files for each image taken at identical spatial positions.

2.1.14. Open the image analysis software. Right click the background to open the window “**Automated Measurement Results**” and “**Automated Measurement**” in the section of “**Analysis Control**”.

2.1.15. In "**Count & Taxonomy**" menu, select "**Count**". On FITC image, click on each nucleus showing green fluorescence (BrdU positive) and right click on the image.

NOTE: The number of BrdU positive cells are shown in the window of "**Automations and Measurements**".

2.1.16. For DAPI images, repeat step 2.1.14 to count the number of total nuclei. Calculate the percentage of BrdU positive cells for this image.

2.1.17. Repeat step 2.1.13 through 2.1.16 for other images for statistical purposes and calculate the mean percentage of BrdU positive cells for each substrate condition.

2.2. Quantification of c-Jun expression through immunofluorescent image analysis

2.2.1. Cells prepared inside 6-well plates from step 1.1.9 and 1.2.23 are fixed and permeabilized with the procedures previously described (step 2.1.5-2.1.7).

NOTE: To perform accurate comparisons of fluorescent intensity across cells of differing ECM conditions, apply camera settings identically across all samples with all samples having the same parameters.

2.2.2. Save images as ".nd2" files.

2.2.3. Open the image analysis software. Right click background to open the window "**Automated Measurement Results**" and "**Automated Measurement**" in the section of "**Analysis Control**".

2.2.4. In "**Automated Measurement Results**", select "**Object Data**". Activate "**Keep updating measurement**" button.

2.2.5. In the top panel of the software, select "**Measure**" followed by "**Object features**". Add "**Mean Intensity**" to the section of "**Selected for Measurement**".

2.2.6. Open and merge two ".nd2" image files that contain images of c-Jun and nuclei.

2.2.7. In the top panel, select "**ROI**" and select "**Draw Rectangular ROI**". Draw a rectangular area containing the nuclear area of a single cell.

NOTE: c-Jun expression is concentrated within nuclei[35].

2.2.8. In top panel of software, select "**Binary**" and "**Define Threshold**", a new window will appear to precisely define c-Jun fluorescent area.

2.2.9. In new window, click "**Full Image/Use ROI**" to switch program from full image model to the ROI model. Use "**Intensity**" to adjust the lookup table located on the left side of the window for adjustment of size/shape of the highlighted area within the rectangular ROI.

NOTE: Take care to ensure the size/shape of the highlighted area is identical to the nucleus.

2.2.10. Click the "**OK**" button, to get the mean FITC intensity in the window of "**Automated Measurement Results**" and then click "**Store Data**".

2.2.11. In the window of "**Automated Measurement**", "**Delete Object**" to remove red highlighted area. On the left side panel, use "**Pointing Tool**" to select the rectangular ROI and delete.

2.2.12. Repeat step 2.2.6 to 2.2.11 to measure mean FITC intensity for each additional cell.

2.2.13. In window area of "**Automated Measurement Results**", select "**Stored**" and all stored data will be presented. Use the "**Export**" function and select "**Data to Excel**" to save the exported spreadsheet and perform additional calculations.

2.3. Quantifying nuclear elongation

2.3.1. Fix and permeabilize SCs prepared from step 1.2.22 following steps 2.1.5-2.1.7. Perform nuclear staining using mounting medium with DAPI.

2.3.2. Using the DAPI channel and a 40x objective lens, acquire images of the sample and save as ".nd2" files.

2.3.3. Follow step 2.2.3 and 2.2.4 to open "**Automated Measurement Results**" and "**Automated Measurement**" window in the image analysis software.

2.3.4. In "**Automated Measurement Results**", use the "**Option**" function followed by "**Select Object Feature**". In the "**Feature**" column, select "**Elongation**" and add to "**Selected for Measurements**" column. Use "**Keep Updating Measurement**" to activate this function.

2.3.5. Open the "nd.2" image file that contains the nuclear images. In "**Automated Measurement**" window, select "**Auto Detect**" function and select a nucleus. Right click on the image and the measured nuclear aspect ratio will be shown in "**Automated Measurement Results**".

2.3.6. Repeat step 2.3.5 to quantify nuclear aspect ratios for other nuclei within the image. Select "**Store Data**" in the window of "**Automated Measurement Results**".

2.3.7. Repeat 2.3.5 to 2.3.6 for additional images. Export the data to a spreadsheet file as previously done in 2.2.13 for analysis.

2.4. Western blot to quantify protein expression

2.4.1. Follow standard protocols for western blot analysis detailed elsewhere[32]. The dilutions of antibodies used in the study are shown below: Rabbit anti c-Jun 1:2,000; Mouse anti β-actin 1:1,000; Rabbit anti p75NTR 1:1,000; Rabbit anti myelin basic protein 1:1,000; Anti-mouse/rabbit IgG, HRP-linked antibody 1:10,000.

REPRESENTATIVE RESULTS:

To analyze and quantify the interplay between substrate stiffness and protein composition on SC phenotype, a tunable PDMS cell culture substrate was developed (**Figure 1A**). Compression testing of the polymer at differing base: curing agent ratios was utilized to quantify the Young's modulus (E) of the substrate (**Figure 1B**). The resulting range of modulus values represents physiologically relevant substrate conditions. Following preparation of substrates, SCs were cultured and cellular properties analyzed on the tunable microenvironment. Proliferation rates of SCs on substrates of differing protein composition were first analyzed. Laminin coated substrates resulted in a higher proliferation rate when compared to collagen I and fibronectin adsorption all at 10 μg/mL (**Figure 2A,B**). SCs on substrates with laminin coating and differing moduli showed that relatively softer substrates (E=3.85kPa) decrease cell proliferation rates across all conditions (**Figure 2C,D**). However, differences between stiff substrates (E=1119kPa) and relatively soft substrates (E=8.67kPa) were insignificant (**Figure 2D**).

SCs were also analyzed for protein expression through immunohistochemistry and western blot. Levels of transcriptional factor c-Jun were analyzed by immunofluorescent microscopy (**Figure 3A**) and represented by the mean pixel fluorescent intensity (**Figure 3B-D**). c-Jun expression was shown to be upregulated as substrates became softer (E=1119 kPa to E=8.67 kPa), however, on the softest substrates (E=3.85 kPa), c-Jun expression was significantly downregulated. On stiff substrates (E=1119 kPa), collagen I coated substrates resulted in the highest c-Jun expression, yet as substrates became softer (E=8.67 kPa and 3.85 kPa), laminin showed the highest levels of c-Jun (**Figure 3E**). Western blot was also used to analyze both c-Jun and myelin basic protein (MBP) with c-Jun levels upregulated and MBP downregulated on softer substrates (**Figure 3F**). Further, SCs seeded on laminin coated substrates resulted in the highest c-Jun expression when compared to collagen I and fibronectin.

Cells of differing seeding densities were then cultured and stained with rhodamine-phalloidin to explore the role of cell spreading and area in c-Jun expression (**Figure 4A,B**). To control nuclear elongation of cells, a common micropatterning technique (microcontact printing[36]) was utilized to create cell adhesive lines on the cell culture substrates. The nuclear aspect ratio of cells seeded on a line patterned substrate was shown to be significantly higher than cells seeded on unpatterned substrates (**Figure 4C,D**). It was found that expression of both c-Jun and another marker significant in SC regenerative phenotypes, p75 neurotrophin receptor (p75 NTR), were upregulated in dense cells with a smaller spreading area (**Figure 4E**). Line-patterned cells also resulted in a higher expression of both c-Jun and p75 NTR when compared to nonpatterned cells (**Figure 4F**). Therefore, microcontact printed cell adhesive geometries were created to precisely

control cell spreading area and elongation while eliminating cell-cell interactions (**Figure 5A**). Dimensions of total cell adhesive areas were 900 μm^2, 1,600 μm^2, and 2,500 μm^2 with an aspect ratio of either 1 or 4 (cell length: cell width). Fluorescent bovine serum albumin (fBSA, Texas red) staining was used to reveal the status of micropatterns on cell culture substrate after microcontact printing (**Figure 5B**). The nuclear aspect ratio of SCs for each cell area was measured and it was shown that by increasing the nuclear aspect ratio, the cellular elongation increases (**Figure 5C**). In addition, as SC aspect ratio increased, c-Jun was upregulated (**Figure 5D**). Interestingly, however, it was found that as cell spreading area increases c-Jun expression is downregulated (**Figure 5E**). Immunofluorescence staining for both nuclei and actin confirmed cell spreading area and elongation were highly controlled through this micropatterning method (**Figure 5F**).

FIGURE LEGENDS:

Figure 1: Cell culture substrates with tunable stiffness and protein composition. (**A**) Schematic showing the development of PDMS cell culture substrates. (**B**) The initial PDMS mixing ratio of base: curing agent determines Young's modulus.

Figure 2: SC proliferation rates regulated by substrate stiffness and protein composition. (**A**) Representative images showing BrdU staining when cultured on substrates of the same modulus. (**B**) Histogram showing the percentage of BrdU positive cells for each protein coating. (**C**) Representative images showing BrdU incorporation in SCs seeded on substrates of the same protein coating. (**D**) Histogram showing the percentage of BrdU positive cells for each Young's modulus value. Scale bars = 50 µm. Data are presented as mean ± SEM. *p < .05, **p < .005, ***p < .0005. Portions of the figure have been modified from ref.[24].

Figure 3: Substrate stiffness and protein regulated SC protein expression. (**A**) Representative images show c-Jun immunofluorescence staining for SCs seeded on substrates of different stiffness and protein composition. Mean pixel fluorescent intensity of c-Jun was measured for SCs seeded on (**B**) collagen I (**C**) fibronectin and (**D**) laminin coated substrates of different stiffness. (**E**) c-Jun fluorescence level of SCs grouped by Young's modulus of substrate. (**F**) Western blot showing c-Jun and myelin basic protein (MBP) of SCs seeded on substrates. Glyceraldehyde 3‐phosphate dehydrogenase (GAPDH) was used as loading control. Scale bar = 50 µm. Data are presented as mean ± SEM. *p < .05, **p < .005, ***p < .0005. Portions of the figure have been modified from ref.[24].

Figure 4: Cellular spreading area influences protein expression of SCs. (**A**) Cell spreading area of different seeding densities was visualized through rhodamine-phalloidin (red) and nuclei staining (blue). (**B**) Histogram showing the average spreading area of SCs in each condition. (**C**) The nuclei of SCs seeded on unpatterned or line-patterned substrates were stained with DAPI (blue) to show morphology. (**D**) Histogram showing quantification of nuclear aspect ratio on patterned and unpatterned substrates. (**E**) Western blot showing expression of c-Jun and p75NTR of cells with different spreading area. (**F**) Western blot showing the protein expression of SCs on unpatterned and line-patterned substrates. Scale bar = 50 µm. Data are presented as mean ± SEM. *p < .05,

**p < .005, ***p < .0005.

Figure 5: SC morphology and elongation impact c-Jun expression of SCs. (**A**) Schematic showing cell micropatterning for shapes of different aspect ratio. (**B**) fBSA staining (red) showing the shape of micropatterns following microcontact printing. Scale bar = 10 μm. (**C**) Histogram showing nuclear aspect ratio of micropatterned SCs. (**D, E**) Histogram showing the mean pixel fluorescent intensity of c-Jun for each of the geometrical conditions. (**F**) Rhodamine-phalloidin (red), nuclei (blue) and c-Jun (green) were stained on the differing micropatterns. Scale bar = 10 μm. Data are presented as mean ± SEM. *p < .05, **p < .005, ***p < .0005. Portions of the figure have been modified from ref.[24].

DISCUSSION:

SCs can promote nerve regeneration due to their phenotypic transformation and regenerative potential following nerve injury. However, how ECM cues regulate this regenerative capacity remains mostly unclear, potentially hindering not only the development of biomaterials that aim to promote nerve regeneration but also the understanding of the mechanisms involved in nerve regeneration. To begin to examine this interplay, cell culture substrates were created where ECM cues such as stiffness, protein coating, and adhesive topography can be controlled. The ability to micropattern adhesive topography is a key feature within the protocol, utilizing the common method of microcontact printing. However, this substrate is different from the glass in that the compression force being applied to the PDMS stamps must be at an appropriate level to achieve the desired shape of cell adhesive areas on cell culture substrates. Utilizing fluorescent bovine serum albumin (fBSA) as a model protein to visualize cell adhesive areas and adjust the compression forces on the PDMS stamps can ultimately mitigate this issue. Another key difference from glass is the removal of excess Pluronic F-127 that is used to render the remainder of the substrate non-adhesive. After this treatment, cell culture substrates are highly hydrophobic, making it challenging to maintain wet cell culture substrates throughout washes, which is important for the structural integrity of micropatterned protein[37]. Therefore, it is recommended to use multiple pipettes to aspirate and inject solutions nearly simultaneously to prevent substrates from completely dehydrating.

Although micropatterning can precisely control cell shape and does not require complicated synthetic procedures using cell blocking polymers such as OEGMA, the methods used to quantify protein expression of micropatterned cells are sometimes limited[38]. For example, samples that are available from micropatterning are generally limited to a few hundred cells per coverslip, which is inadequate to prepare cell lysates to be used for western blots or qPCR. Considering this, immunofluorescence staining alone was used to quantify protein expression for micropatterned cells, limiting the variety of proteins that can be quantified. To address this, we utilized line patterns to promote cell elongation for larger cell populations and successfully prepared cell lysates that were analyzed by western blot. Other methods such as applied electric fields or aligned electrospun fibers can also be applied to control the elongation of cell populations[39,40]. However, electric fields may not fit into all applications for NGCs since the conductivity of commonly used biomaterials such as collagen-based polymer and silk is very low[28,41,42]. In contrast, aligned electrospun nanofibers have been successfully implanted into NGCs to promote

SC alignment, elongation and migration as well as neurite outgrowth[43,44]. It may also prove compelling to compare SC behavior on line-patterned substrates against those on substrates with aligned nanofibers, since lined patterns and aligned nanofibers are two of the most common guidance mechanisms incorporated into NGCs[45].

The micropatterning protocol detailed utilizes PDMS coated coverslips as cell culture substrates, with a maximum surface Young's modulus of 1119 kPa. Such stiffness mimics many tissue, yet it may not be possible to model osteogenesis of mesenchymal stem cells, which generally require the surface Young's modulus to exceed 1 Gpa[46]. For such situations, glass is an alternative candidate, however the adsorption of Pluronic F-127 requires relatively high surface hydrophobicity which glass does not possess. To increase hydrophobicity, glass can be treated with dimethyl dichlorosilane in dichlorobenzene. Following this, UV-Ozone treatment can be used to increase hydrophilicity for microcontact printing[47].

Ultimately, a cell culture platform was developed where ECM stimuli can be tuned individually with protein expression quantified. We have determined that SC regenerative capacity is promoted by certain mechanical and chemical ECM cues, which can subsequently provide inspiration in the future design of biomaterial applications such as NGCs and cell transplantation processes where ECM features may need to be optimized[24]. Nonetheless, tuning these ECM cues can be a challenging undertaking, particularly in vivo. Moving forward, this platform can be utilized to parse key mechanisms involved in the phenotypic transition of SCs as regulated by the ECM. By achieving this, manipulation of intracellular cues may be possible to promote SC regenerative capacity without the need for dedicated platforms in vitro[48,49]. This has the potential for groundbreaking work in the development of technologies for nerve repair.

ACKNOWLEDGMENTS:

The authors gratefully acknowledge funding support from the University of Cincinnati. The authors also thank Ron Flenniken of the University of Cincinnati Advanced Materials Characterization laboratory for support.

DISCLOSURES:

No potential conflict of interest was reported by the authors.

REFERENCES:

1. Taylor, C. A., Braza, D., Rice, J. B., Dillingham, T. The Incidence of Peripheral Nerve Injury in Extremity Trauma. *American Journal of Physical Medicine & Rehabilitation.* **87**, 381-385 (2008).
2. Noble, J., Munro, C. A., Prasad, V. S. S. V., Midha, R. Analysis of Upper and Lower Extremity Peripheral Nerve Injuries in a Population of Patients with Multiple Injuries. *Journal of Trauma and Acute Care Surgery.* **45**, 116-122 (1998).
3. Jessen, K. R., Mirsky, R. The repair Schwann cell and its function in regenerating nerves. *Journal of Physiology.* **594**, 3521-3531 (2016).
4. Arthur-Farraj, P. J. et al. c-Jun Reprograms Schwann Cells of Injured Nerves to Generate a Repair Cell Essential for Regeneration. *Neuron.* **75**, 633-647 (2012).
5. Jessen, K. R., Mirsky, R. The Success and Failure of the Schwann Cell Response to Nerve

659 Injury. *Frontiers in Cell Neurosciences.* **13**, 33 (2019).
660 6. Gomez-Sanchez, J. A. et al. After Nerve Injury, Lineage Tracing Shows That Myelin and
661 Remak Schwann Cells Elongate Extensively and Branch to Form Repair Schwann Cells, Which
662 Shorten Radically on Remyelination. *Journal of Neuroscience.* **37** (37), 9086-9099 (2017).
663 7. Deumens, R. et al. Repairing injured peripheral nerves: Bridging the gap. *Progress in*
664 *Neurobiology.* **92**, 245-276 (2010).
665 8. Höke, A., Gordon, T., Zochodne, D. W., Sulaiman, O. A. R. A decline in glial cell-line-derived
666 neurotrophic factor expression is associated with impaired regeneration after long-term
667 Schwann cell denervation. *Experimental Neurology.* **173**, 77-85 (2002).
668 9. Jones, S., Eisenberg, H. M., Jia, X. Advances and future applications of augmented
669 peripheral nerve regeneration. *International Journal of Molecular Sciences.* **17**, 1-17 (2016).
670 10. Harris, G. M. et al. Nerve Guidance by a Decellularized Fibroblast Extracellular Matrix.
671 *Matrix Biology.* **60-61**, 176-189 (2017).
672 11. Harris, G. M., Piroli, M. E., Jabbarzadeh, E. Deconstructing the Effects of Matrix Elasticity
673 and Geometry in Mesenchymal Stem Cell Lineage Commitment. *Advanced Function Mater.* **24**
674 (16), 2396-2403 (2014).
675 12. Pryzhkova, M. V., Harris, G. M., Ma, S., Jabbarzadeh, E. Patterning pluripotent stem cells
676 at a single cell level. *Journal of Biomaterials and Tissue Engineering.* **3** (4), 461-471 (2013).
677 13. Engler, A. J., Sweeney, H. L., Discher, D. E., Schwarzbauer, J. E. Extracellular matrix
678 elasticity directs stem cell differentiation. *Journal of Musculoskeleton and Neuronal Interaction.*
679 **7** (4), 335 (2007).
680 14. Chen, C. S., Mrksich, M., Huang, S., Whitesides, G. M., Ingber, D. E. Geometric control of
681 cell life and death. *Science.* **276** (5317), 1425-1428 (1997).
682 15. Engler, A. J., Sen, S., Sweeney, H. L., Discher, D. E. Matrix Elasticity Directs Stem Cell
683 Lineage Specification. *Cell.* **126**, 677-689 (2006).
684 16. Pickup, M. W., Mouw, J. K., Weaver, V. M. The extracellular matrix modulates the
685 hallmarks of cancer. *EMBO Reports.* **15**, 1243-1253 (2014).
686 17. Chernousov, M. A., Carey, D. J. Schwann cell extracellular matrix molecules and their
687 receptors. *Histology and Histopathology.* **15**, 593-601 (2000).
688 18. Shibata, S. et al. Selective Laminin-Directed Differentiation of Human Induced Pluripotent
689 Stem Cells into Distinct Ocular Lineages. *Cell Reports.* **25** (6), 1668-1679 (2018).
690 19. Mcbeath, R., Pirone, D. M., Nelson, C. M., Bhadriraju, K., Chen, C. S. Cell Shape,
691 Cytoskeletal tenstion and RhoA regulate stem cell lineage committment. *Developmental Cell.* **6**,
692 483-495 (2004).
693 20. Halder, G., Dupont, S., Piccolo, S. Transduction of mechanical and cytoskeletal cues by
694 YAP and TAZ. *Nature Reviews Molecular Cell Biology.* **13**, 591-600 (2012).
695 21. Jessen, K. R., Mirsky, R. The repair Schwann cell and its function in regenerating nerves.
696 *Journal of Physiology.* **594** (13), 3521-3531 (2016).
697 22. Lopez-Fagundo, C., Bar-Kochba, E., Livi, L. L., Hoffman-Kim, D., Franck, C. Three-
698 dimensional traction forces of Schwann cells on compliant substrates. *Journal of The Royal*
699 *Society Interface.* **11**, 20140247-20140247 (2014).
700 23. Gu, Y. et al. The influence of substrate stiffness on the behavior and functions of Schwann
701 cells in culture. *Biomaterials.* **33**, 6672-6681 (2012).
702 24. Xu, Z. Y., Orkwis, J. A., DeVine, B. M., Harris, G. M. Extracellular matrix cues modulate

703 Schwann cell morphology, proliferation, and protein expression. *Journal of Tissue Engineering*
704 *and Regenerative Medicine.* 10.1002/term.2987, (2019).
705 25. Urbanski, M. M. et al. Myelinating glia differentiation is regulated by extracellular matrix
706 elasticity. *Scientific Reports.* **6**, 1-12 (2016).
707 26. Sun, Y. et al. Tunable stiffness of graphene oxide/polyacrylamide composite scaffolds
708 regulates cytoskeleton assembly. *Chemical Sciences.* **9** (31), 6516-6522 (2018).
709 27. Hwang, J. H. et al. Extracellular matrix stiffness regulates osteogenic differentiation
710 through MAPK activation. *PLoS One.* **10**, 1-16 (2015).
711 28. Ryan, A. J. et al. A Physicochemically Optimized and Neuroconductive Biphasic Nerve
712 Guidance Conduit for Peripheral Nerve Repair. *Advanced Healthcare Materials.* **6**, 1-13 (2017).
713 29. Du, J. et al. Prompt peripheral nerve regeneration induced by a hierarchically aligned
714 fibrin nanofiber hydrogel. *Acta Biomaterialia.* **55**, 296-309 (2017).
715 30. Huang, L. et al. A compound scaffold with uniform longitudinally oriented guidance cues
716 and a porous sheath promotes peripheral nerve regeneration in vivo. *Acta Biomaterialia.* **68**, 223-
717 236 (2018).
718 31. Brower, K., White, A. K., Fordyce, P. M. Multi-step Variable Height Photolithography for
719 Valved Multilayer Microfluidic Devices. *Jouranl of Visualized Experiments.* (119), e55276 (2017).
720 32. Gupta, R. et al. Shear stress alters the expression of myelin-associated glycoprotein (MAG)
721 and myelin basic protein (MBP) in Schwann cells. *Journal of Orthopaedic Research : Official*
722 *Publication of the Orthopaedic Research Society.* **23**, 1232-1239 (2005).
723 33. Harris, G. M., Shazly, T., Jabbarzadeh, E. Deciphering the combinatorial roles of geometric,
724 mechanical, and adhesion cues in regulation of cell spreading. *PLoS One.* **8** (11), (2013).
725 34. Engler, A. J., Sen, S., Sweeney, H. L., Discher, D. E. Matrix elasticity directs stem cell lineage
726 specification. *Cell.* **126** (4), 677-689 (2006).
727 35. Schreck, I. et al. C-Jun localizes to the nucleus independent of its phosphorylation by and
728 interaction with JNK and vice versa promotes nuclear accumulation of JNK. *Biochemical and*
729 *Biophysical Research Communications.* **407**, 735-740 (2011).
730 36. Shen, K., Qi, J., Kam, L. C. Microcontact printing of proteins for cell biology. *Journal*
731 *Visualized Experiments.* (22), e1065 (2008).
732 37. Treter, J. et al. Washing-resistant surfactant coated surface is able to inhibit pathogenic
733 bacteria adhesion. *Applied Surface Science.* **303**, 147-154 (2014).
734 38. Lutz, J.-F. Polymerization of oligo(ethylene glycol) (meth)acrylates: Toward new
735 generations of smart biocompatible materials. *Journal of Polymer Science Part A: Polymer*
736 *Chemistry.* **46** (11), 3459-3470 (2008).
737 39. Marcus, M. et al. Interactions of Neurons with Physical Environments. *Advanced*
738 *Healthcare Materials.* **6**, (2017).
739 40. Pu, J. Golgi polarization in a strong electric field. *Journal of Cell Science.* **118**, 1117-1128
740 (2005).
741 41. Blaker, J. J. et al. Bioactive Silk-Based Nerve Guidance Conduits for Augmenting Peripheral
742 Nerve Repair. *Advanced Healthcare Materials.* **7**, 1800308 (2018).
743 42. Daly, W., Yao, L., Zeugolis, D., Windebank, A., Pandit, A. A biomaterials approach to
744 peripheral nerve regeneration : bridging the peripheral nerve gap and enhancing functional
745 recovery. *Journal of the Royal Society of Interface.* **9** (67) 202-221, (2012).
746 43. Xia, H. et al. Directed neurite growth of rat dorsal root ganglion neurons and increased

colocalization with Schwann cells on aligned poly(methyl methacrylate) electrospun nanofibers. *Brain Research.* **1565**, 18-27 (2014).
44. Wang, H. B., Mullins, M. E., Cregg, J. M., McCarthy, C. W., Gilbert, R. J. Varying the diameter of aligned electrospun fibers alters neurite outgrowth and Schwann cell migration. *Acta Biomaterialia.* **6**, 2970-2978 (2010).
45. Carvalho, C. R., Oliveira, J. M., Reis, R. L. Modern Trends for Peripheral Nerve Repair and Regeneration: Beyond the Hollow Nerve Guidance Conduit. *Frontiers in Bioengineering and Biotechnology.* **7**, 337, (2019).
46. Yang, Y., Wang, K., Gu, X., Leong, K. W. Biophysical Regulation of Cell Behavior — Cross Talk between Substrate Stiffness and Nanotopography. *Engineering.* **3**, 36-54 (2017).
47. Tan, J. L., Liu, W., Nelson, C. M., Raghavan, S., Chen, C. S. Simple Approach to Micropattern Cells on Common Culture Substrates by Tuning Substrate Wettability. *Tissue Engineering.* **10**, 865-872 (2004).
48. Grove, M. et al. YAP/TAZ initiate and maintain schwann cell myelination. *Elife.* **6**, 1-27 (2017).
49. Poitelon, Y. et al. YAP and TAZ control peripheral myelination and the expression of laminin receptors in Schwann cells. *Nature Neuroscience.* **19**, 879-887 (2016).

Figure 1

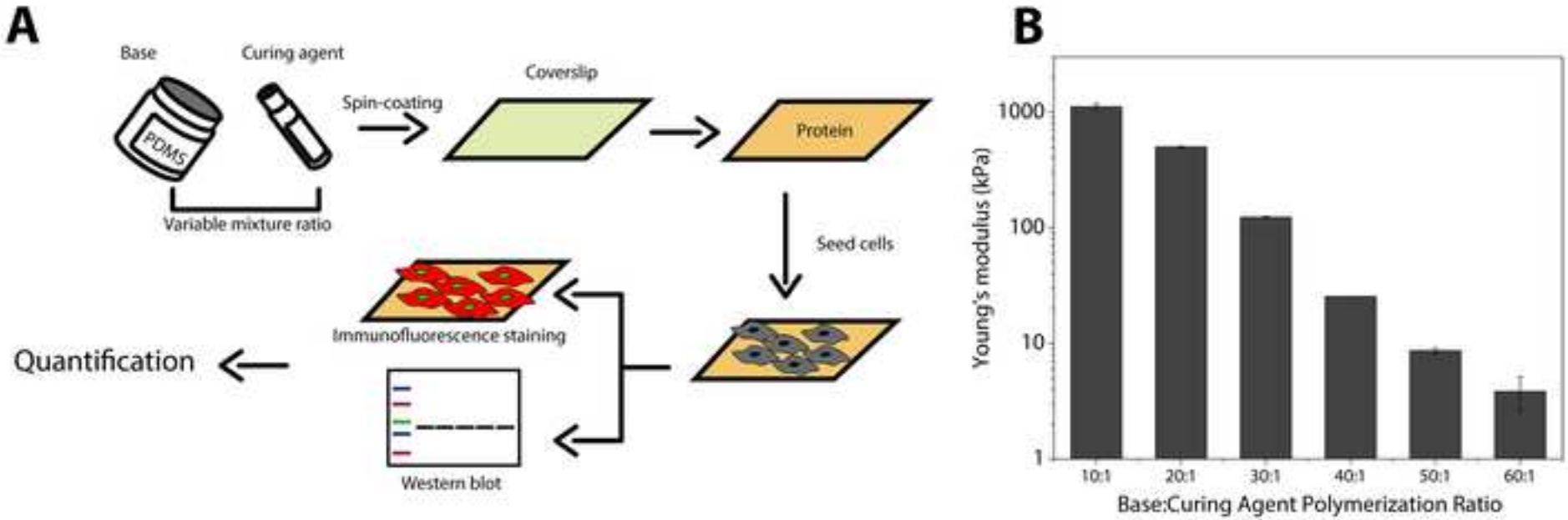

Figure 2

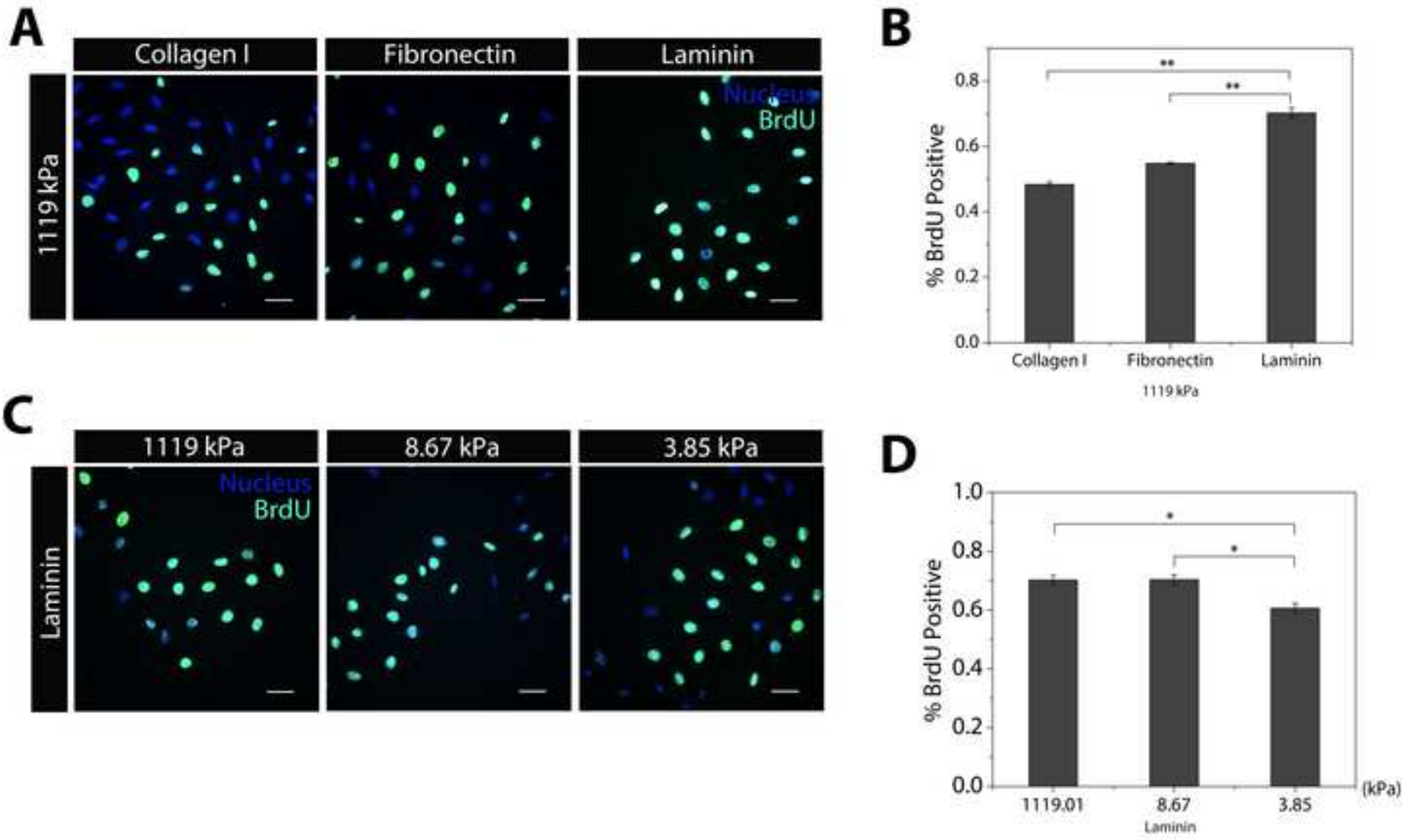

Figure 3

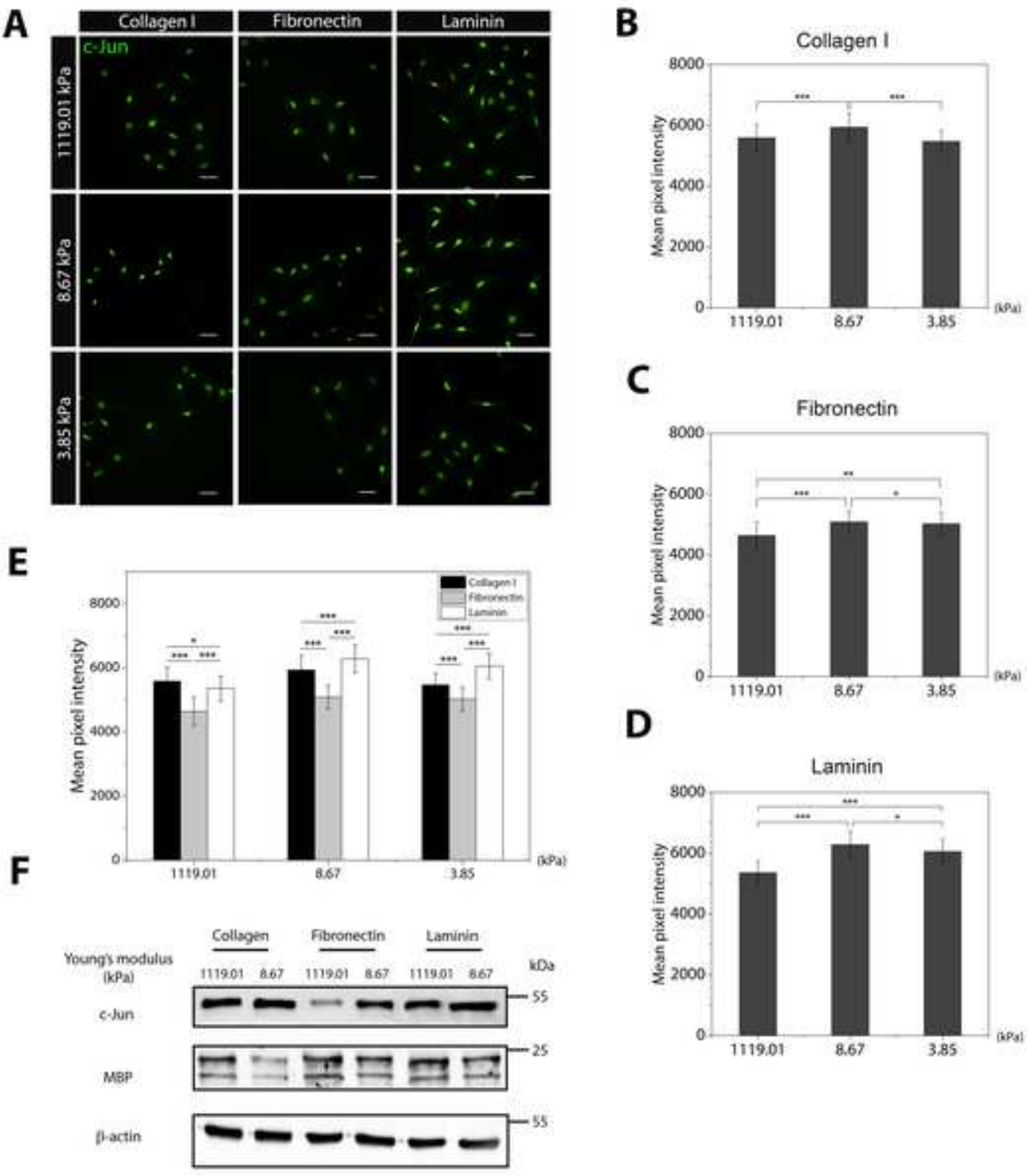

Figure 4

Click here to access/download;Figure;Figure 4.tif

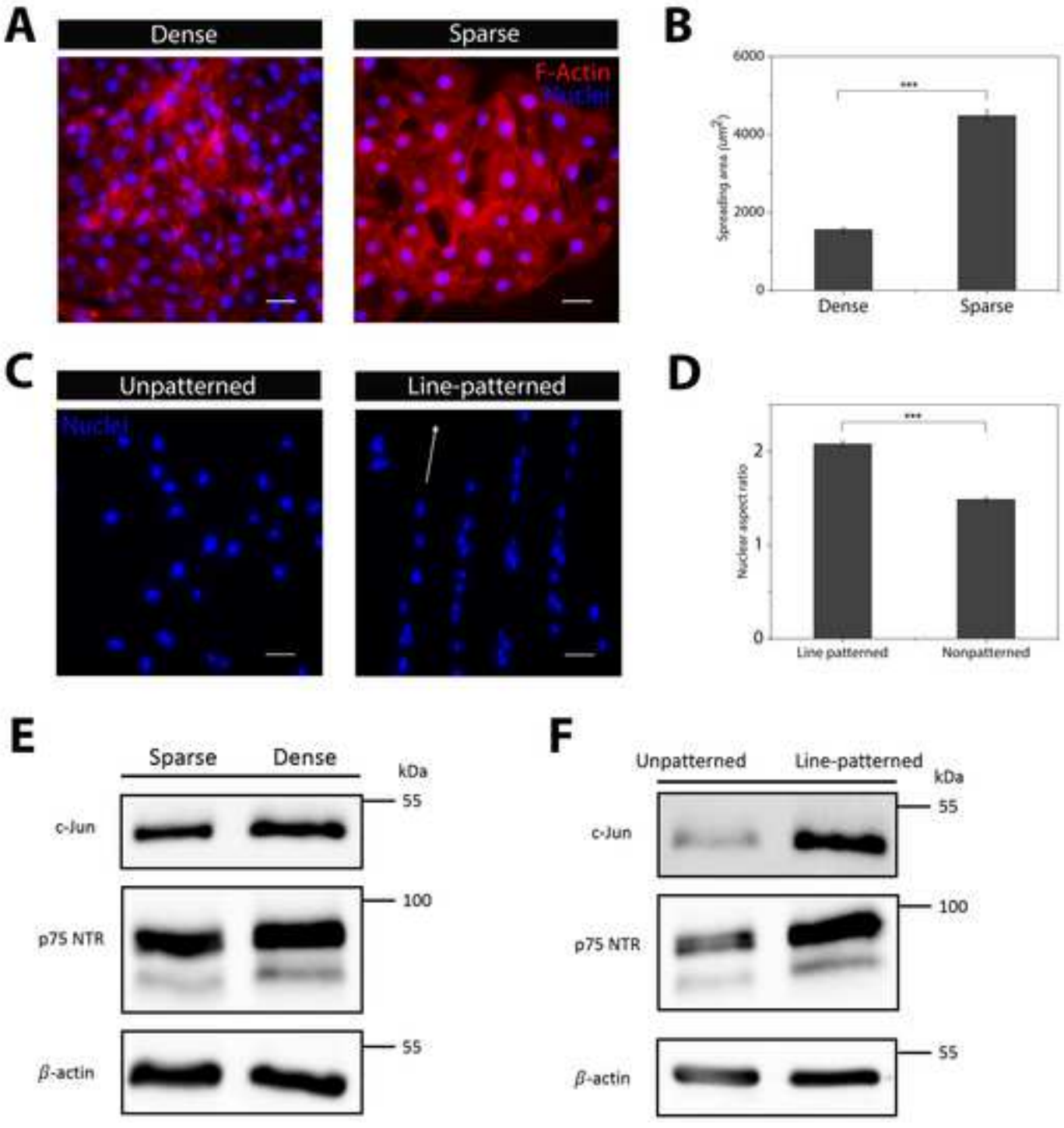

Figure 5

Click here to access/download;Figure;Figure 5.tif

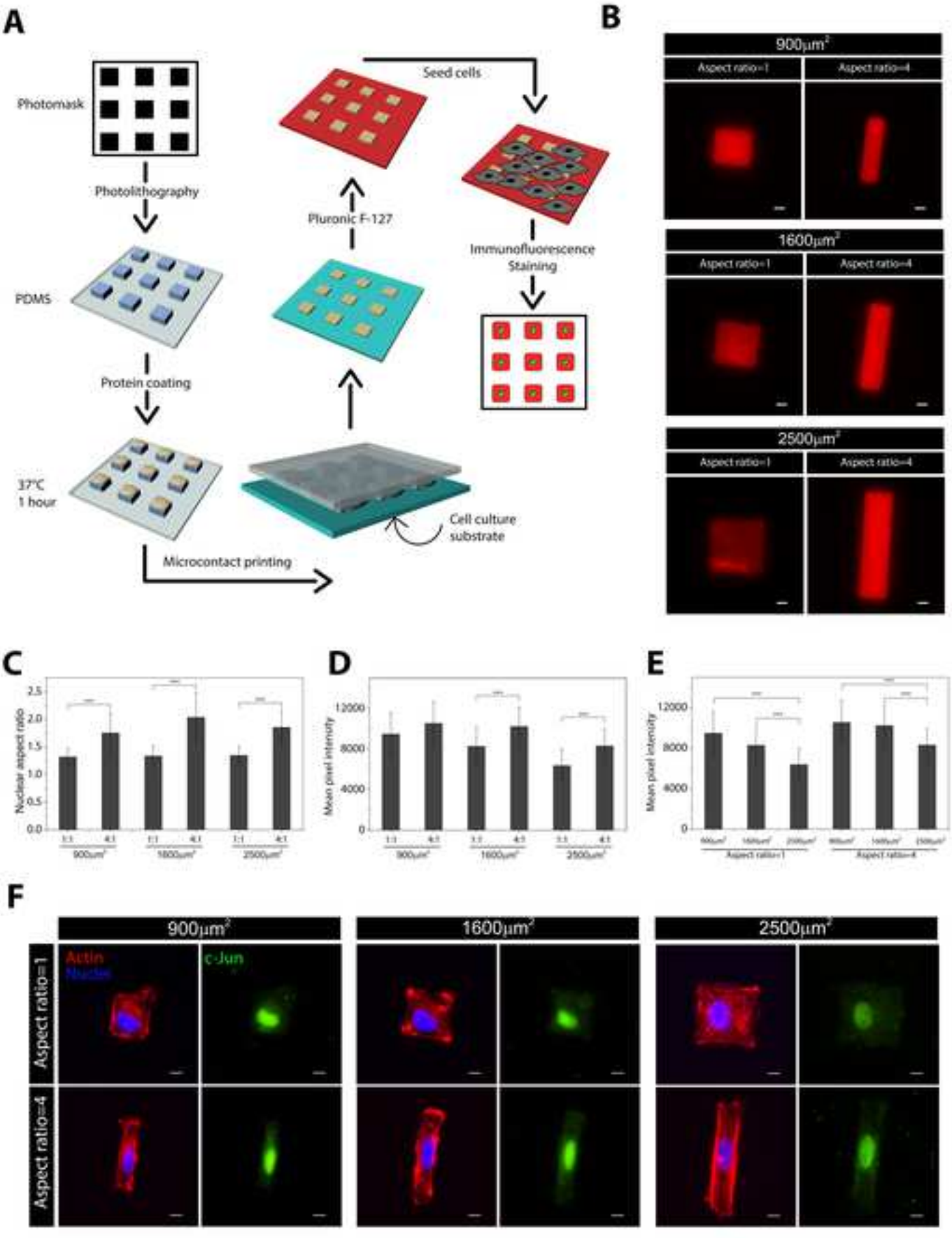

Table of Materials

Name of Material/ Equipment	Company	Catalog Number	
Albumin from Bovine Serum (BSA), Texas Red conjugate	Thermo Fisher Scientific	A23017	
Anti-mouse IgG, HRP-linked Antibody	Cell Signaling Technology	7076S	
Anti-rabbit IgG, HRP-linked Antibody	Cell Signaling Technology	7074S	
BrdU	Thermo Fisher Scientific	B23151	
BrdU primary antibody conjugated with Alexa Fluor 488	Thermo Fisher Scientific	B35130	
Collagen I	Thermo Fisher Scientific	A10483-01	
Compression force test machine	TestResources		Ir
Dulbecco's Modified Eagle Medium	Thermo Fisher Scientific	11965092	
Fetal Bovine Serum	Thermo Fisher Scientific	16000044	
Fibronectin	Thermo Fisher Scientific	33010-018	
Fluorescence microscope	Nikon	Eclipse Ti2	
Halt Protease and Phosphatase Inhibitor Cocktail (100X)	Thermo Fisher Scientific	78440	
Laminin	Thermo Fisher Scientific	23017015	
Mounting medium with DAPI	Thermo Fisher Scientific	P36971	
Mouse c-Jun primary antibody	Thermo Fisher Scientific	711202	
Mouse β-Actin primary antibody	Cell Signaling Technology	3700S	

Penicillin-Streptomycin	Thermo Fisher Scientific	15140122
Photoresist SU 2010	KAYAKU	SU8-2010
Pluronic F-127	Sigma Aldrich	P-2443
Rabbit c-Jun primary antibody	Cell Signaling Technology	9165S
Rabbit myelin basic protein primary antibody	Abcam	ab40390
Rabbit p75NTR primary antibody	Cell Signaling Technology	8238S
Rhodamine phalloidin	Thermo Fisher Scientific	R415
RIPA buffer	Abcam	ab156034
RT4-D6P2T Schwann cell line	ATCC	CRL-2768
SYLGARD 184 PDMS base and curing agent	Sigma Aldrich	761036
Trypsin	Thermo Fisher Scientific	15090-046
UV-Ozone cleaner	Novascan	
Versene (1x)	Thermo Fisher Scientific	15040066

Comments/Description
BSA staining to show micropatterns
Antibody used for western blot analysis
Antibody used for western blot analysis
Reagent used to measure cell proliferation
Used to visualize BrdU in cell proliferation assays
Protein used to coat coverslips
ıstrument to quantify mechanical properties of polymers
Cell culture medium
Cell culture medium supplemental
Protein used to coat coverslips
Fluorescence microscope
Protease and Phosphatase Inhibitor
Protein used to coat coverslips
Coverslip mountant and nuclei staining
Primary antibody to visualize c-Jun protein
Loading control for western blot experiments

Cell culture medium supplemental

Photoresist

Block non-specific protein binding

Primary antibody for visualization of c-Jun protein

Primary antibody for visualization of MBP

Primary antibody for visualization of p75NTR

Visualization of cell cytoskeleton

Cell lysis buffer

Cell line used in experiments

Tunable polymer used to coat coverslips

Cell dissociation reagent

Increase hydrophicility of PDMS

Cell dissociation reagent

JoVE61496
RESPONES TO REVIEWERS

The authors would like to thank the reviewers for their time and effort in reviewing and improving this protocol. The suggestions from reviewers have been addressed as follows:

Reviewer #1:

1. Based on the study of Schwann cells, why did you choose the Young's Modulus of 1119kPa to screen proteins instead of the Young's Modulus similar to neural tissue?

PDMS (Polydimethylsiloxane) mixed with curing agent at a mixing ratio of 10:1 resulted in a surface Young's modulus of 1119kPa. This is a common mixing ratio for PDMS in biological studies and has been used previously in many different publications[1-3]. Furthermore, we attempted to determine how Schwann cells (SCs) would respond when seeded on substrates across a spectrum of matrix stiffness values, as opposed to a substrate with one specific stiffness value.. In addition, we went to modulus values lower than that found in peripheral nerve to cover the spectrum of peripheral nerve matrix modulus, as seen in our results where the "optimal" stiffness for Schwann cells is 8.67 kPa (ref 24 from protocol).

2. What are the criteria for screening three Young's modulus in the experiment?

This protocol describes the methods based on our recent publication[4]. In this work, we seeded SCs on substrates with Young's modulus (E) values of approximately 1119, 502.35, 123.89, 25.51, 8.67 and 3.85 kPa. After analysis, we determined that several critical SC behaviors such as proliferation and key phenotypic protein expression can be promoted when substrate stiffness decreased from 1119 kPa to 8.67 kPa, however little change in the values from 119 kPa to 8.67 kPa was observed. In addition, SC proliferation rates and certain protein levels declined as substrates became even softer (3.85 kPa) from 8.67 kPa. These results indicated that 1119, 8.67 and 3.85 kPa are three important demarcations for Young's moduli within our study values, so these three Young's moduli were chosen as the representative results for the protocol.

3. In Figure 3, the protein results of the 3.85 kPa group in the experimental need to be supplemented.

We did not highlight the western blot results for the 3.85 kPa group because in our recent publication which this protocol is based upon, we performed western blot analysis for c-Jun and myelin basic protein (MBP) of SCs seeded on uncoated PDMS (PDMS that is not coated with any protein), therefore there were no available gel lanes to run electrophoresis for a 3.85 kPa group of this protein, and in the interest of rigor regarding western blots, were left out. However, fluorescent staining clearly showed c-Jun fluorescent intensity was significantly lower for 3.85 kPa group compared to 8.67 kPa, which is strong evidence that the western blot for the 3.85 kPa group would show similar results and we believe with this available data our results establish our claims.

4. The micropattern status after PDMS stamp microcontact printing is not shown in the results.

The authors agree and this oversight has been amended. The micropatterning status on cell culture substrates following printing have been added by incorporating microcontact printed fluorescent bovine serum albumin (fBSA) in new Figure 5B showing protein on the surface.

5. The abscissa in Figure 5E is incorrect.

The abscissa has been corrected.

6. In the quantification of cellular properties on tunable substrates experiment, why not culture the cells directly on the flexible PDMS stamp with the protein adsorbed?

We elected not to seed cells directly on PDMS stamps due to the following key reasons among others:

(A) By culturing cells directly on the flexible PDMS stamps, it would introduce physical barriers as a variable to cellular function. As cells would be trapped inside the channels, variability would be introduced into the tunable culture system.

(B) For a repeatable protocol, it is more difficult to scrape cells and collect cell lysates when cells are seeded onto PDMS stamps with physical barriers surrounding cells compared to cells seeded on PDMS coated petri dishes.

(C) PDMS with lower Young's moduli such as 8.67 and 3.85 kPa are difficult to handle during experiments. The PDMS is fairly "sticky" and prone to dust attachment, which is not ideal for cell culture and can lead to user error. By making a stamp and printing onto a spincoated PDMS surface, it eliminates these variables.

(D) If SCs had been seeded on PDMS stamps, in order to preserve samples for microscopy, PDMS stamps would need to be sealed on coverslips with nail polish. This would require us to make PDMS stamps repeatedly, thereby consuming more PDMS than our current method of making a thin layer on aglass coverslip. Seeding cells on PDMS coated substrates instead of PDMS stamps is especially helpful in terms of cell micropatterning since it enables researchers to use one PDMS stamp over several experiments. Without making PDMS stamps repeatedly the patterns on the silicon master can be better preserved.

7.It may be more appropriate to use the mean pixel intensity on the unit surface to evaluate the c-jun factor.

Mean pixel intensity was used to quantify c-Jun fluorescent intensity. "MeanIntensity" which measures the mean pixel intensity of region of interest (ROI), was added to measurements (see red rectangle in

Figure 1)

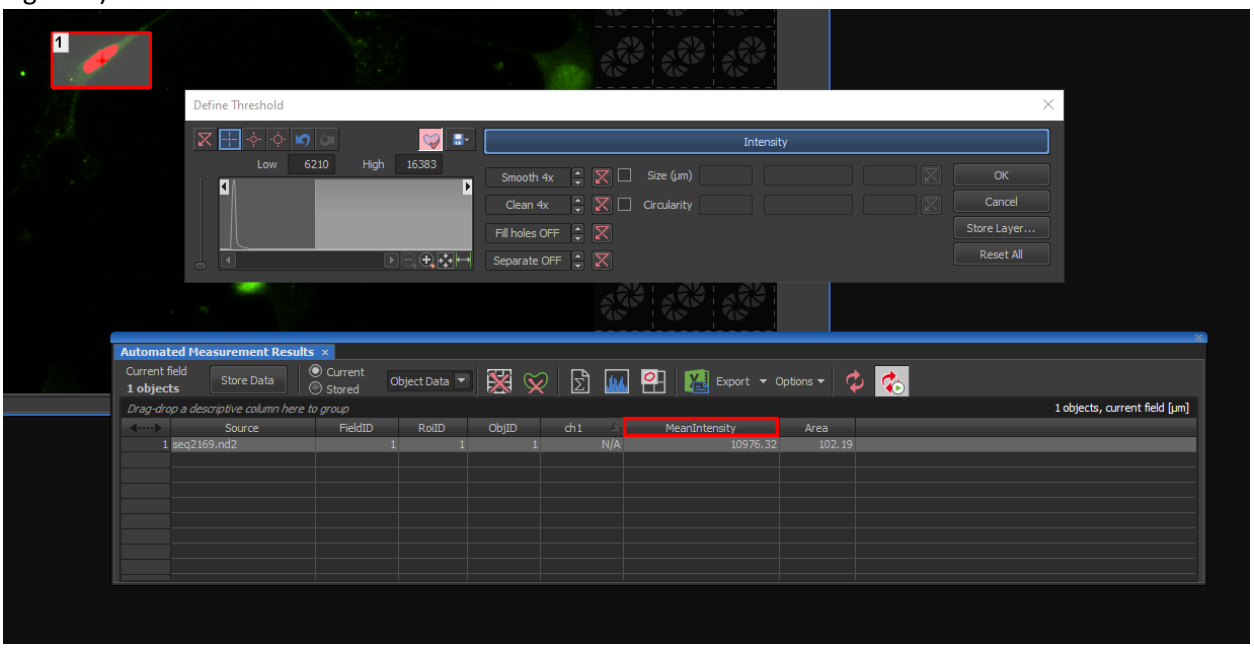

Figure 1 A screen shot shows we used mean pixel intensity to quantify c-Jun expression level across different substrates.

8. Fig.2, images of A 1119kPa-Lamin and Fig.2C Lamin-3.85kPa are the same?

Those two images represented the SCs seeded on the same chemical (laminin coated) and physical (Young's modulus =1119 kPa) condition, so the same representative image was used. However, to resolve this issue, we have replaced the representative image for the third panel of Figure 2A.

Reviewer #2:

1. It is known that the media conditions change SC phenotype, there are no details about the media composition used for cultivating SCs, this should be added.

The media composition has been added to step 1.1.9.

2. What is a curing agent used for?

There are two components to the PDMS (Polydimethyl siloxane) system as received: one a base elastomer and the other a curing agent. During polymerization, the curing agent crosslinks with base elastomer to impart mechanical integrity to the liquid precursors. Specific to our experiment, we adjusted the crosslink ratio between base elastomer and curing agent to create PDMS with different stiffnesses to be used as cell culture substrates. The function of the curing agent has been clarified in the note following step 1.1.1.

3. The explanation on what the Pluronic solution is used for comes only during the discussion, while it should also be explained earlier in the protocol.

The function of Pluronic F-127 was explained in a note following step 1.2.13.

4. In the protocol section, even id trivial the purpose of each reagent is often missing:

PFA for fixation (lane 2.1.5), triton X-100 for permeabilization (lane 318), HCl citric acid buffer for antigen retrieval (lane 320-325), BSA…

The manuscript has been updated to explain the function of formaldehyde in step 2.1.5, the function of Triton X-100 in step 2.1.6, the function of HCl treatment within proliferation assay in the note following step 2.1.8, the function of phosphate/citric acid buffer in step 2.1.9, and the function of BSA in step 2.1.10.

5. Figure3A. It is unfortunate that the image representing increase in proliferation rates with laminin is also showing fewer cells overall, is there any cellular death? A better representative image should be used to better convey the results.

The proliferation rate of SCs was calculated using an average percentage of BrdU positive cells over 70 images for each cell culture condition, the randomly chosen representative images in Figure 3A happened to be an area with fewer cells. To address this issue, we have replaced the representative images in Figure 3A.

6. While the section 2.4 refers to the ref 32 for Western blot and protein quantification, the protein extraction method should be detailed as the obtention of a sufficient protein yield might be challenging due to the specific experimental condition of the method; with cell spreading/ low density.

The SC lysis protocol has been added to the manuscript following step 1.2.23.

7. The micropatterning technique used to study the SC nuclear elongation is not very well introduced. The authors need to speak about the bands of Büngner to clarify why creating cell adhesive lines is a great tool to mimic SC environment during nerve regeneration.

The relationship between line patterned substrates and elongated SCs inside Büngner bands has been more adequately explained in the fourth paragraph of the introduction.

References

1 Srinivasan, A. *et al.* Microchannel-based regenerative scaffold for chronic peripheral nerve interfacing in amputees. *Biomaterials.* **41** 151-165, (2015).

2 Jacchetti, E., Tonazzini, I., Meucci, S., Beltram, F. & Cecchini, M. Microstructured polydimethylsiloxane membranes for peripheral nerve regeneration. *Microelectronic Engineering.* **124** 26-29, (2014).
3 Brown, X. Q., Ookawa, K. & Wong, J. Y. Evaluation of polydimethylsiloxane scaffolds with physiologically-relevant elastic moduli: Interplay of substrate mechanics and surface chemistry effects on vascular smooth muscle cell response. *Biomaterials.* **26** 3123-3129, (2005).
4 Xu, Z., Orkwis, J. A., DeVine, B. M. & Harris, G. M. Extracellular matrix cues modulate Schwann cell morphology, proliferation, and protein expression. *J Tissue Eng Regen Med.* 10.1002/term.2987, (2019).

JOHN WILEY AND SONS LICENSE
TERMS AND CONDITIONS

May 05, 2020

This Agreement between University of Cincinnati -- Greg Harris ("You") and John Wiley and Sons ("John Wiley and Sons") consists of your license details and the terms and conditions provided by John Wiley and Sons and Copyright Clearance Center.

License Number	4822540691609
License date	May 05, 2020
Licensed Content Publisher	John Wiley and Sons
Licensed Content Publication	Journal of Tissue Engineering and Regenerative Medicine
Licensed Content Title	Extracellular matrix cues modulate Schwann cell morphology, proliferation, and protein expression
Licensed Content Author	Zhenyuan Xu, Jacob A. Orkwis, Braden M. DeVine, et al
Licensed Content Date	Nov 14, 2019
Licensed Content Volume	14
Licensed Content Issue	2
Licensed Content Pages	14
Type of use	Journal/Magazine

Requestor type	Author of this Wiley article
Is the reuse sponsored by or associated with a pharmaceutical or medical products company?	no
Format	Electronic
Portion	Figure/table
Number of figures/tables	3
Will you be translating?	No
Circulation	50000 or greater
Title of new article	Deciphering the Impact of ECM in Schwann Cell Phenotype Specification
Lead author	Zhenyuan Xu
Title of targeted journal	JoVE
Publisher	JoVE
Expected publication date	Sep 2020
Order reference number	JoVE_Manuscript
Portions	Figure 2A,C,D,E has been modified with different representative images and different graphing. Figure 3 has been modified with different representative images and different western blot. Figure 6A has been modified with different representative images.
Requestor Location	University of Cincinnati 2901 Woodside Drive

846 Engineering Research Center

Cincinnati, OH 45221
United States
Attn: University of Cincinnati

Publisher Tax ID EU826007151

Total 0.00 USD

Terms and Conditions

TERMS AND CONDITIONS

This copyrighted material is owned by or exclusively licensed to John Wiley & Sons, Inc. or one of its group companies (each a"Wiley Company") or handled on behalf of a society with which a Wiley Company has exclusive publishing rights in relation to a particular work (collectively "WILEY"). By clicking "accept" in connection with completing this licensing transaction, you agree that the following terms and conditions apply to this transaction (along with the billing and payment terms and conditions established by the Copyright Clearance Center Inc., ("CCC's Billing and Payment terms and conditions"), at the time that you opened your RightsLink account (these are available at any time at http://myaccount.copyright.com).

Terms and Conditions

- The materials you have requested permission to reproduce or reuse (the "Wiley Materials") are protected by copyright.
- You are hereby granted a personal, non-exclusive, non-sub licensable (on a stand-alone basis), non-transferable, worldwide, limited license to reproduce the Wiley Materials for the purpose specified in the licensing process. This license, **and any CONTENT (PDF or image file) purchased as part of your order,** is for a one-time use only and limited to any maximum distribution number specified in the license. The first instance of republication or reuse granted by this license must be completed within two years of the date of the grant of this license (although copies prepared before the end date may be distributed thereafter). The Wiley Materials shall not be used in any other manner or for any other purpose, beyond what is granted in the license. Permission is granted subject to an appropriate acknowledgement given to the author, title of the material/book/journal and the publisher. You shall also duplicate the copyright notice that appears in the Wiley publication in your use of the Wiley Material. Permission is also granted on the understanding that nowhere in the text is a previously published source acknowledged for all or part of this Wiley Material. Any third party content is expressly excluded from this permission.
- With respect to the Wiley Materials, all rights are reserved. Except as expressly granted by the terms of the license, no part of the Wiley Materials may be copied, modified, adapted (except for minor reformatting required by the new Publication), translated, reproduced, transferred or distributed, in any form or by any means, and no

derivative works may be made based on the Wiley Materials without the prior permission of the respective copyright owner.**For STM Signatory Publishers clearing permission under the terms of the STM Permissions Guidelines only, the terms of the license are extended to include subsequent editions and for editions in other languages, provided such editions are for the work as a whole in situ and does not involve the separate exploitation of the permitted figures or extracts,** You may not alter, remove or suppress in any manner any copyright, trademark or other notices displayed by the Wiley Materials. You may not license, rent, sell, loan, lease, pledge, offer as security, transfer or assign the Wiley Materials on a stand-alone basis, or any of the rights granted to you hereunder to any other person.

- The Wiley Materials and all of the intellectual property rights therein shall at all times remain the exclusive property of John Wiley & Sons Inc, the Wiley Companies, or their respective licensors, and your interest therein is only that of having possession of and the right to reproduce the Wiley Materials pursuant to Section 2 herein during the continuance of this Agreement. You agree that you own no right, title or interest in or to the Wiley Materials or any of the intellectual property rights therein. You shall have no rights hereunder other than the license as provided for above in Section 2. No right, license or interest to any trademark, trade name, service mark or other branding ("Marks") of WILEY or its licensors is granted hereunder, and you agree that you shall not assert any such right, license or interest with respect thereto

- NEITHER WILEY NOR ITS LICENSORS MAKES ANY WARRANTY OR REPRESENTATION OF ANY KIND TO YOU OR ANY THIRD PARTY, EXPRESS, IMPLIED OR STATUTORY, WITH RESPECT TO THE MATERIALS OR THE ACCURACY OF ANY INFORMATION CONTAINED IN THE MATERIALS, INCLUDING, WITHOUT LIMITATION, ANY IMPLIED WARRANTY OF MERCHANTABILITY, ACCURACY, SATISFACTORY QUALITY, FITNESS FOR A PARTICULAR PURPOSE, USABILITY, INTEGRATION OR NON-INFRINGEMENT AND ALL SUCH WARRANTIES ARE HEREBY EXCLUDED BY WILEY AND ITS LICENSORS AND WAIVED BY YOU.

- WILEY shall have the right to terminate this Agreement immediately upon breach of this Agreement by you.

- You shall indemnify, defend and hold harmless WILEY, its Licensors and their respective directors, officers, agents and employees, from and against any actual or threatened claims, demands, causes of action or proceedings arising from any breach of this Agreement by you.

- IN NO EVENT SHALL WILEY OR ITS LICENSORS BE LIABLE TO YOU OR ANY OTHER PARTY OR ANY OTHER PERSON OR ENTITY FOR ANY SPECIAL, CONSEQUENTIAL, INCIDENTAL, INDIRECT, EXEMPLARY OR PUNITIVE DAMAGES, HOWEVER CAUSED, ARISING OUT OF OR IN CONNECTION WITH THE DOWNLOADING, PROVISIONING, VIEWING OR USE OF THE MATERIALS REGARDLESS OF THE FORM OF ACTION, WHETHER FOR BREACH OF CONTRACT, BREACH OF WARRANTY, TORT, NEGLIGENCE, INFRINGEMENT OR OTHERWISE (INCLUDING, WITHOUT LIMITATION, DAMAGES BASED ON LOSS OF PROFITS, DATA, FILES, USE, BUSINESS OPPORTUNITY OR CLAIMS OF THIRD PARTIES), AND WHETHER OR NOT THE PARTY HAS BEEN ADVISED OF THE POSSIBILITY OF SUCH DAMAGES. THIS LIMITATION SHALL APPLY NOTWITHSTANDING ANY FAILURE OF ESSENTIAL PURPOSE OF ANY LIMITED REMEDY PROVIDED

HEREIN.

- Should any provision of this Agreement be held by a court of competent jurisdiction to be illegal, invalid, or unenforceable, that provision shall be deemed amended to achieve as nearly as possible the same economic effect as the original provision, and the legality, validity and enforceability of the remaining provisions of this Agreement shall not be affected or impaired thereby.

- The failure of either party to enforce any term or condition of this Agreement shall not constitute a waiver of either party's right to enforce each and every term and condition of this Agreement. No breach under this agreement shall be deemed waived or excused by either party unless such waiver or consent is in writing signed by the party granting such waiver or consent. The waiver by or consent of a party to a breach of any provision of this Agreement shall not operate or be construed as a waiver of or consent to any other or subsequent breach by such other party.

- This Agreement may not be assigned (including by operation of law or otherwise) by you without WILEY's prior written consent.

- Any fee required for this permission shall be non-refundable after thirty (30) days from receipt by the CCC.

- These terms and conditions together with CCC's Billing and Payment terms and conditions (which are incorporated herein) form the entire agreement between you and WILEY concerning this licensing transaction and (in the absence of fraud) supersedes all prior agreements and representations of the parties, oral or written. This Agreement may not be amended except in writing signed by both parties. This Agreement shall be binding upon and inure to the benefit of the parties' successors, legal representatives, and authorized assigns.

- In the event of any conflict between your obligations established by these terms and conditions and those established by CCC's Billing and Payment terms and conditions, these terms and conditions shall prevail.

- WILEY expressly reserves all rights not specifically granted in the combination of (i) the license details provided by you and accepted in the course of this licensing transaction, (ii) these terms and conditions and (iii) CCC's Billing and Payment terms and conditions.

- This Agreement will be void if the Type of Use, Format, Circulation, or Requestor Type was misrepresented during the licensing process.

- This Agreement shall be governed by and construed in accordance with the laws of the State of New York, USA, without regards to such state's conflict of law rules. Any legal action, suit or proceeding arising out of or relating to these Terms and Conditions or the breach thereof shall be instituted in a court of competent jurisdiction in New York County in the State of New York in the United States of America and each party hereby consents and submits to the personal jurisdiction of such court, waives any objection to venue in such court and consents to service of process by registered or certified mail, return receipt requested, at the last known address of such party.

WILEY OPEN ACCESS TERMS AND CONDITIONS

Wiley Publishes Open Access Articles in fully Open Access Journals and in Subscription journals offering Online Open. Although most of the fully Open Access journals publish open access articles under the terms of the Creative Commons Attribution (CC BY) License only, the subscription journals and a few of the Open Access Journals offer a choice of Creative Commons Licenses. The license type is clearly identified on the article.

The Creative Commons Attribution License

The Creative Commons Attribution License (CC-BY) allows users to copy, distribute and transmit an article, adapt the article and make commercial use of the article. The CC-BY license permits commercial and non-

Creative Commons Attribution Non-Commercial License

The Creative Commons Attribution Non-Commercial (CC-BY-NC)License permits use, distribution and reproduction in any medium, provided the original work is properly cited and is not used for commercial purposes.(see below)

Creative Commons Attribution-Non-Commercial-NoDerivs License

The Creative Commons Attribution Non-Commercial-NoDerivs License (CC-BY-NC-ND) permits use, distribution and reproduction in any medium, provided the original work is properly cited, is not used for commercial purposes and no modifications or adaptations are made. (see below)

Use by commercial "for-profit" organizations

Use of Wiley Open Access articles for commercial, promotional, or marketing purposes requires further explicit permission from Wiley and will be subject to a fee.

Further details can be found on Wiley Online Library
http://olabout.wiley.com/WileyCDA/Section/id-410895.html

Other Terms and Conditions:

v1.10 Last updated September 2015

Questions? customercare@copyright.com or +1-855-239-3415 (toll free in the US) or +1-978-646-2777.

JoVE61496
RESPONES TO EDITORS

Editorial comments:

1. Please take this opportunity to thoroughly proofread the manuscript to ensure that there are no spelling or grammar issues. The JoVE editor will not copy-edit your manuscript and any errors in the submitted revision may be present in the published version.

Everything has been checked and no spelling or grammatical errors can be found.

2. Please format the manuscript as: paragraph Indentation: 0 for both left and right and special: none, Line spacings: single. Please include a single line space between each step, substep and note in the protocol section. Please use Calibri 12 points

The manuscript has been formatted according to editor's instructions.

3. Please provide an email address for each author.

The email address for each author has been provided.

4. Please ensure that all text in the protocol section is written in the imperative tense as if telling someone how to do the technique (e.g., "Do this," "Ensure that," etc.). The actions should be described in the imperative tense in complete sentences wherever possible. Avoid usage of phrases such as "could be," "should be," and "would be" throughout the Protocol. Any text that cannot be written in the imperative tense may be added as a "Note."

The manuscript has been checked and the whole protocol section is written in the imperative tense.

5. The Protocol should contain only action items that direct the reader to do something.

All descriptive content within protocol section has been deleted or written as a "Note".

6. Please ensure that individual steps of the protocol should only contain 2-3 actions sentences per step.

We have split steps that contain more than 3 actions into multiple steps, for example step 1.1.8, 1.2.18, 1.3.3 and 2.2.3.

7. Please use S.I. abbreviations throughout the manuscripts: h, min, s, etc.

The units have been corrected.

8. Please adjust the numbering of the Protocol to follow the JoVE Instructions for Authors. For example, 1 should be followed by 1.1 and then 1.1.1 and 1.1.2 if necessary. Please refrain from using bullets, alphabets, or dashes.

The bullets have been deleted and the contents have been integrated into the text. The numbering has been checked and adjusted following the JoVE Instructions for Authors.

9. Please add more details to your protocol steps. Please ensure you answer the "how" question, i.e., how is the step performed?

More details have been added to the protocol section for a better illustration. For example, steps 1.1.8, 1.1.9, 1.2.13, 1.2.17, 2.1.5, 2.1.6, 2.1.8, 2.1.9 and 2.1.10 better explain the protocol. We also added steps that detail SC lysate preparation for line-patterned Schwann cells (SCs) starting on step 1.2.20.1.

10. There is a 10-page limit for the Protocol, but there is a 2.75-page limit for filmable content. Please highlight 2.75 pages or less of the Protocol (including headings and spacing) that identifies the essential steps of the protocol for the video, i.e., the steps that should be visualized to tell the most cohesive story of the Protocol.

The highlighted protocol has been shortened to comply the guideline provided by the journal.

11. Please obtain explicit copyright permission to reuse any figures from a previous publication. Explicit permission can be expressed in the form of a letter from the editor or a link to the editorial policy that allows re-prints. Please upload this information as a .doc or .docx file to your Editorial Manager account. The Figure must be cited appropriately in Figure Legend, i.e. "This figure has been modified from [citation]."

Copyright permission for modified figures has been uploaded

12. Please ensure the result are described in the context of your experiment, you performed an experiment, how did it help you to conclude what you wanted to and how is it in line with the title.

The outcome of all experimental protocols is shown in "results" and "figures" section. In detail, step 1.1, which described the process of preparing tunable substrates, was shown in Figure 1A. Step 1.2, which demonstrated SC micropatterning, was shown in Figures 4 and 5. Step 1.3, which demonstrated the method to measure Young's moduli of PDMS substrates, was shown in Figure 1B. Step 2.1 which discussed the proliferation assay and immunofluorescence staining, corresponds to Figure 2, 3, 4, and 5. Step 2.2, which details c-Jun fluorescent intensity measurement, corresponds to Figure 3. Step 2.3 demonstrates nuclear elongation quantification, was shown in Figure 4D and 5C.

13. As we are a methods journal, please ensure the Discussion explicitly cover the following in detail in 3-6 paragraphs with citations:
a) Critical steps within the protocol
b) Any modifications and troubleshooting of the technique
c) Any limitations of the technique
d) The significance with respect to existing methods
e) Any future applications of the technique

We have addressed the above critical points thoroughly in the discussion section. The first paragraph explicitly discusses critical steps within this protocol regarding SC micropatterning. Then we discuss using fluorescent bovine serum albumin (fBSA) staining to aid in applying the appropriate force on PDMS stamps as a troubleshooting method for SC micropatterning. The second paragraph discusses the limitation of SC micropatterning, which is protein expression quantification. We have also compared current techniques that can promote SC elongation such as electric fields and aligned electrospun fibers with line patterns. In the third paragraph of discussion, we presented a potential modification to micropattern cell adhesive areas on glass substrates. In the fourth paragraph

of the discussion, we discuss the future clinical applications of our study that focused on tunable substrates and SC micropatterning.

14. Figure 2A third panel and Figure 2C first panel are same. Please check

Those two images represented the SCs seeded on the same chemical (laminin coated) and physical (Young's modulus =1119 kPa) condition, so the same representative image was used. To resolve this issue, we replaced the representative image for the third panel of Figure 2A.

15. Figure 5: X-axis title are reversed.

The title of the X-axis has been fixed.